



J. Serb. Chem. Soc. 85 (2) 203–214 (2020)
JSCS–5294

A binary copper(II) complex having a stepped polymeric structure: Synthesis, characterization, DNA-binding and anti-fungal studies

MUHAMMAD IQBAL^{1*}, SAQIB ALI^{2**}, MUHAMMAD N. TAHIR³, MUHAMMAD ABDUL HALEEM¹, HUSSAIN GULAB¹ and NASEER ALI SHAH⁴

¹Department of Chemistry, Bacha Khan University, Charsadda 24420, KPK, Pakistan,

²Department of Chemistry, Quaid-i-Azam University, Islamabad 45320, Pakistan,

³Department of Physics, University of Sargodha, Sargodha, Pakistan and ⁴Department of Biosciences, Islamabad Campus, COMSATS University Islamabad, Park Road, Islamabad, Pakistan

(Received 23 April, revised 19 June, accepted 24 June 2019)

Abstract: A rarely found polymeric complex of copper(II) was obtained in the reaction of 2-(4-methylphenyl)acetate and copper sulfate and crystallized in quantitative yield. The complex was characterized using FT-IR, electron spin resonance, absorption spectroscopy, electrochemistry and powder and single crystal XRD studies. The structure was found to consist of interconnected paddlewheel units without an intervening ligand resulting in a stepped polymeric arrangement of the structure. The purity of the sample was judged from powder XRD data while ESR spectroscopy indicated a weak signal between 3000 and 4000 G values, indicating the presence of Cu(II) in the complex. Electrochemistry revealed an irreversible, predominantly diffusion controlled $\text{Cu}^{\text{II}}\text{Cu}^{\text{II}}/\text{Cu}^{\text{II}}\text{Cu}^{\text{I}}$ process with a D_0 value calculated to be $3.032 \times 10^{-8} \text{ cm}^2 \text{ s}^{-1}$. The complex was screened for its DNA-binding ability through cyclic voltammetry, absorption and fluorescence spectroscopy and viscometry; the former two yielding K_b values of 3.34×10^3 and $6.90 \times 10^3 \text{ M}^{-1}$, respectively. The complex exhibited significant activity against fungal strain *Mucor piriformis*, moderate activity against *Aspergillus niger* and slight activity against *Helminthosporium solani*. These preliminary findings revealed the excellent biological potential of the synthesized complex.

Keywords: polymeric Cu(II) complex; structure; DNA-binding; antifungal activity.

*** Corresponding authors. E-mail: (*)iqbalmo@yahoo.com, iqbal@bkuc.edu.pk;
(**)saqibali@qau.edu.pk
<https://doi.org/10.2298/JSC190423065I>

INTRODUCTION

The most commonly encountered structure of copper(II) carboxylates is the paddlewheel type in which four carboxylate ligands act as simple bidentate, bridging the two copper centers in the *syn-syn* configuration. The inter-dinuclear distance within this binuclear entity is usually around 2.6 Å, which is somewhat longer than the covalent bond between Cu and axially bonded N, O and F atoms.¹ This shorter distance is due to the geometrical restraints imposed by the four bridging bonds between the two copper ions. Due to the shorter distance, a crystallography program (used for drawing the structure of a complex) usually draws a bond between the two copper ions of the paddlewheel structure. However, this bond is meaningless because the unpaired electron on the copper(II) ion is in the $d_{x^2-y^2}$ -orbital, which is oriented towards the bridging Cu–O bonds rather than the other Cu(II) ion within the paddlewheel unit. Hence a meaningful overlap is impossible along the axis joining the two copper ions. In contrast, the d_{z^2} -orbital can participate in such an overlap between the two copper ions of the dinuclear unit but these orbitals are filled on both ions. For these reasons, there is no bond between the copper centers in a paddlewheel unit and the geometry of each copper ion is square pyramidal if the copper is axially coordinated by another ligand.²

If both copper ions of the paddlewheel unit are coordinated axially by monodentate ligands, the resulting structure is a discrete paddlewheel molecule.³ However, there are complexes having interlinked paddlewheel units in which the binuclear units are *trans*-interlinked *via* copper, oxygen or both atoms by intervening ligands. There is great structural diversity of such polynuclear paddlewheel complexes.⁴ In another type of complexes, the paddlewheel units are interconnected with their own copper and oxygen atoms without the intervention of other ligands. This type is not as much widespread and few examples have been reported so far.⁵ Moreover, ample studies on the properties of such polymeric complexes have not been conducted.⁵ The arrangement of paddlewheel units in this type is almost linear having a stepped polymeric structure.

Copper is part of several enzymes and coenzymes and plays the key role in crucial biochemical reactions. Owing to its bio-essentiality, its complexes are expected to be less toxic compared to the observed toxic side effects of the currently used platinum-based anticancer drugs.⁶ Moreover, it has been found that one of the causes of the toxic behavior of platinum based drugs is their covalent and irreversible binding with cellular DNA of the target tissue.⁷ In this context, any newly designed bioactive drug is desired to bind with DNA in a non-covalent binding mode. Thus, the DNA-binding activity is a preliminary test along with antimicrobial activity after synthesis and characterization of a metal-based complex destined for biological activities.⁸ In the present study, a copper(II) complex related to the less commonly found polymeric type of paddlewheel

complexes has been synthesized and isolated. This complex was structurally characterized and its DNA-binding as well as antimicrobial properties explored.

EXPERIMENTAL

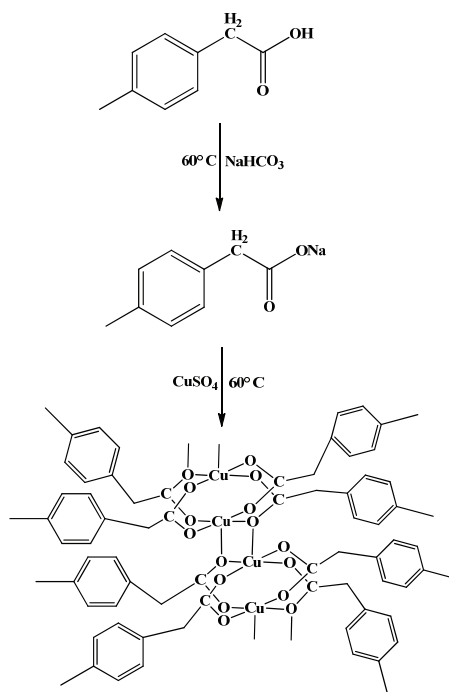
Chemicals and methods

The analytical grade materials used in this work were purchased from suppliers. The melting point was determined on an electrothermal apparatus and the FT-IR spectra were recorded on a Nicolet-6700 spectrophotometer fitted with an ATR. Powder XRD data was acquired using a PANalytical, X'Pert PRO diffractometer having Cu K_{α} radiation ($\lambda = 1.540598 \text{ \AA}$) at 298 K. The X-band electron spin resonance (ESR) spectrum was obtained using a Bruker ESP-300 spectrometer having X-band frequency $\sim 9.5 \text{ GHz}$.

The experimental protocols of single crystal XRD study, electrochemistry, absorption and fluorescence spectroscopy, viscosity measurement and antifungal studies are given in the Supplementary material to this paper.

Synthesis of the complex

Sodium bicarbonate (0.504 g, 6 mmol) was reacted with an equimolar quantity of 2-(4-methylphenyl)acetic acid (6 mmol, 0.90 g) at $60 \text{ }^{\circ}\text{C}$ in distilled water, as shown in Scheme 1. After complete neutralization of the acid with the base, an aqueous solution of copper sulphate (0.240 g, 3 mmol) was added dropwise. The reaction mixture was stirred for 4 h at $60 \text{ }^{\circ}\text{C}$ and the resulting precipitate was filtered, washed thoroughly with distilled water and air dried. The solid was recrystallized from a mixture of chloroform and methanol (1:1) as blue crystals in a yield of 60 %; m.p. $208\text{--}209 \text{ }^{\circ}\text{C}$.



Scheme 1. Synthetic procedure to the complex.

RESULTS AND DISCUSSION

A copper(II) complex has been isolated and crystallized in a good yield and characterized by the melting point, FT-IR, electron spin resonance, UV-Vis spectroscopy, electrochemistry and powder and single crystal XRD techniques.

FT-IR study

The most important peaks are given in the Supplementary material. In the FT-IR spectrum, the asymmetric and symmetric stretching vibrations of the carboxylate moiety of the complex were observed at 1612 and 1382 cm^{-1} . This gives rise to a $\Delta\nu$ value of 230 cm^{-1} , which is typical of the bridging bidentate coordination mode of the carboxylate ligand, in support of the findings from single crystal XRD. Another important peak of low intensity was observed at 422 cm^{-1} that is assignable to the stretching of a Cu–O bond, which indicated the bonding of the ligand to copper through oxygen. Similarly, other peaks, such as C=C, Ar–H, methyl–C–H and methylene–C–H stretching vibrations, were observed in their usual regions. The FT-IR spectrum of the crystalline sample revealed all the important peaks, which were supportive of other characterization techniques.

Electron spin resonance spectroscopy

A weak ESR signal was indicated between 3000 and 4000 G values as shown in Fig. 1A. This range is typical of copper(II) complexes⁹ and the ESR signal indicated a copper(II) center in the sample of the complex. The weak response in the ESR might be the reason for the relatively few magneto-structural studies conducted on such polymeric complexes.⁵

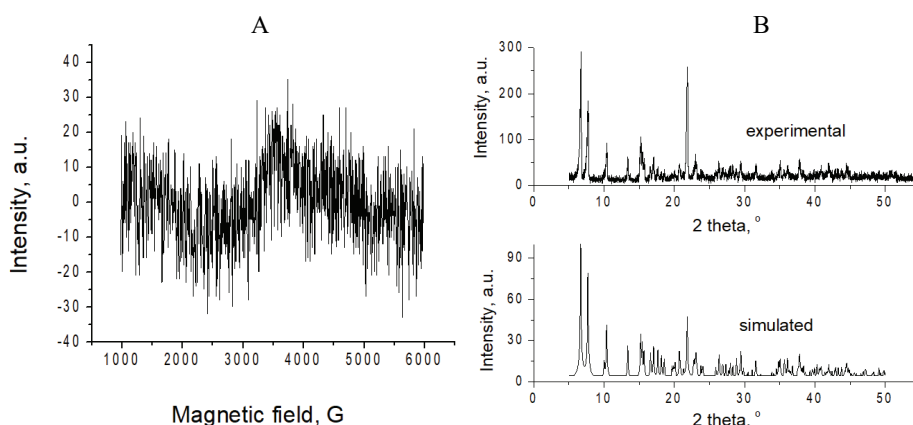


Fig. 1. A – X-Band ESR spectrum of the complex and B – experimental and simulated powder XRD spectra of the complex showing coincidence of the peaks on 2θ values.

Powder XRD study

Being NMR-silent, the bulk purity of the crystalline sample of the copper(II) complex was ascertained from its XRD spectra (powder and single crystal). The powder X-ray diffraction spectrum of the synthesized complex was obtained and compared with the respective simulated spectrum of the complex by superimposing the spectra. The experimental and simulated powder XRD spectra agree mutually, as shown in Fig. 1B, indicating that the complex was isolated and crystallized in completely pure form.

Crystal structure description of the complex

Molecular structure of the complex (poly{tetrakis[2-(4-methylphenyl)acetato- μ -O,O']dicopper(II)}) is shown in Fig. 2 and its crystal refinement parameters and bond distances are listed in Tables I and S-I. The supramolecular structure of the complex consists of 1D layers interlinked through C–H \cdots C interactions, as shown in Fig. 3 in which each molecule represents a 1D layer.

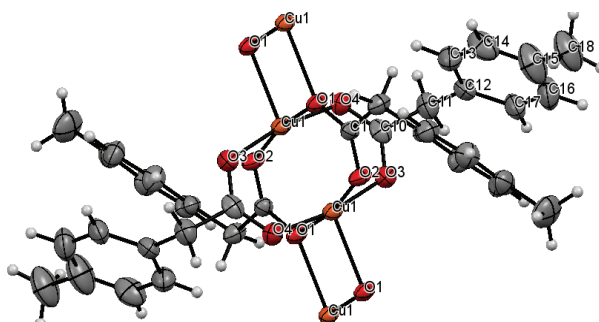


Fig 2. Structure of a paddlewheel unit of the complex poly{tetrakis[2-(4-methylphenyl)acetato- μ -O,O']dicopper(II)} with atom numbering scheme.

TABLE I. Selected bond lengths and angles of the complex

Bond	Distance, Å	Bond	Angle, °
Cu(1)–O(1)	2.007(2)	O(4)–Cu(1)–O(1)	88.15(11)
Cu(1)–O(2)	1.968(2)	O(2)–Cu(1)–O(3)	88.17(11)
Cu(1)–O(3)	1.941(3)	O(1)–Cu(1)–O(2)	169.28(9)
Cu(1)–O(1)	2.239(2)	O(4)–Cu(1)–O(3)	169.45(10)
Cu(1)–O(4)	1.941(3)	O(1)–Cu(1)–O(3)	91.20(11)
Cu(1)–Cu(1)	2.5962(8)	O(4)–Cu(1)–O(2)	90.51(11)
		O(1)–Cu(1)–O(3)	95.46(10)
		O(4)–Cu(1)–O(1)	94.72(10)
		O(1)–Cu(1)–O(2)	112.33(9)
		O(1)–Cu(1)–O(1)	78.39(10)

The structure is composed of interconnected (through Cu–O bonds) paddlewheel units in an almost linear fashion resulting in a 1D polymeric chain (Fig. 4).

Within a paddlewheel unit, the two copper ions are mutually bonded by four 1,2-carboxylic linkages. These four Cu–O bonds around each Cu(II) form the square base of the square pyramidal geometry around each copper the apical position of which is formed by oxygen of the next paddlewheel unit of the polymeric chain. Since the ligands are same and the metal to ligand ratio is 1:2, the structure is homolyptic.

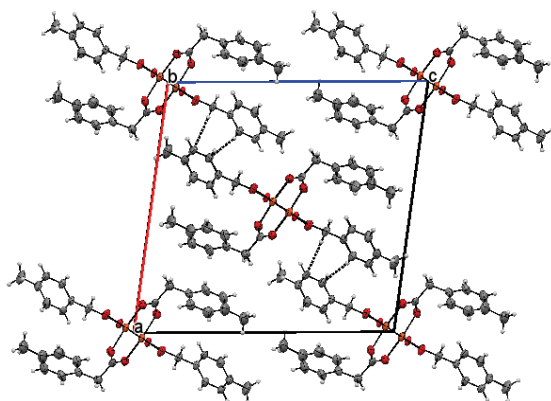


Fig. 3. Packing diagram of the complex in which each molecule represents a 1D-layer. The layers are held together by C···H–C interactions.

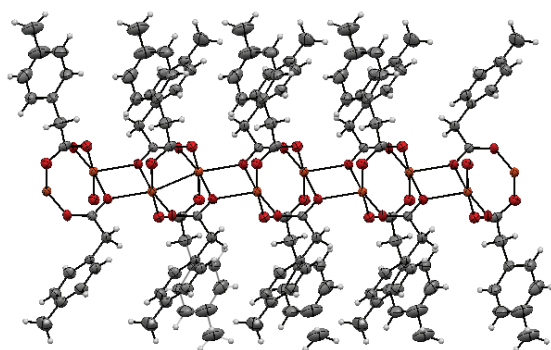


Fig. 4. Stepped structure of a 1D layer of the polymeric complex.

The Cu···Cu distance within the paddlewheel unit is 2.596 Å, which is not much longer than the usual Cu–O/N/F bond lengths. However, this short distance is indicative of the geometrical restraint imposed by the four carboxylate bonds between the two copper ions. There is no bond between the two ions. The out of plane nature of the copper ion from the basal plane may also be the result of this restraint as it is typical of other paddlewheel structures.¹⁰ The Cu···Cu bond distance was found to vary with the nature of the bonds around the Cu, whereby soft donor atoms around copper were found to have longer Cu···Cu separation.¹¹ The apical Cu–O bond (2.240 Å) is longer than the equatorial Cu–O bonds (average = 1.9642 Å) owing to the double electron occupancy of the d_{z^2} orbital lying on the apical axis.

Electrochemical study

The solution behavior of the complex was assessed using cyclic voltammetry that yielded a voltammogram consisting of widely spaced (145 mV) couple of oxidation (13 mV) and reduction (−132 mV) signals (shown in Fig. 5) attributable to the $\text{Cu}^{\text{II}}\text{Cu}^{\text{II}}/\text{Cu}^{\text{II}}\text{Cu}^{\text{I}}$ process. The metal-based oxidation and reduction processes around zero potential value indicated the facile electron transfer reaction of the Cu(II) ion. This behavior and peak ranges are typical of those observed for structurally similar copper(II) complex.¹⁰ Some insight into the electron transfer reaction was obtained from a logarithmic plot of current and scan rate, the linearity with a slope value of 0.3 indicated a diffusion-controlled process in the three-electrode cell.¹² A parameter of prime importance in a diffusion controlled process is the diffusion coefficient D_0 , the value of which is determined using Randles–Sevcik equation.¹³ Using the slope value of current vs. square root of scan rate plot (shown in Fig. S-1), in association with the Bard and Faulkner equation,¹⁴ the value of D_0 was calculated to be $3.032 \times 10^{-8} \text{ cm}^2 \text{ s}^{-1}$.

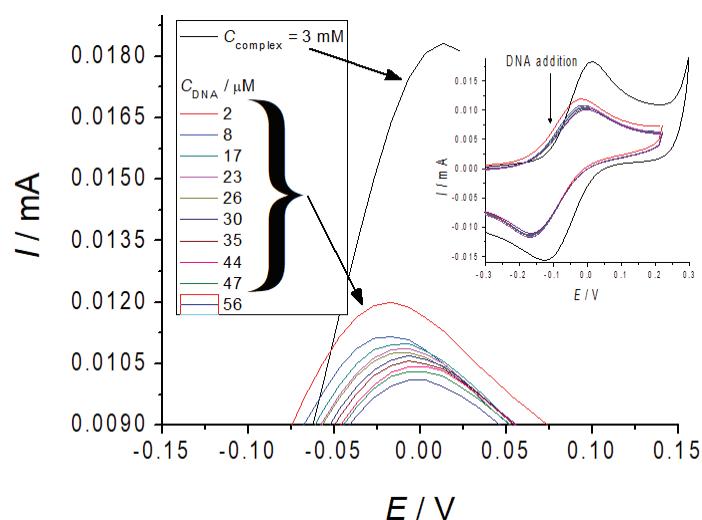


Fig. 5. Clarified oxidation peak of the complex at 100 mV s^{-1} before (uppermost peak) and after addition of DNA (lower, shifted peaks). The inset shows the complete voltammograms.

Absorption spectroscopy

The light blue colored solution of the complex gave rise to a metal centered broad absorption band corresponding to the d–d transition of the Cu(II) ion (d^9 configuration) in the wavelength range 550–950 nm, as shown in Fig. 6A. This absorption spectrum corresponds to excitation from ${}^2B_{1g}$ and the fact that the $d_{x^2-y^2}$ orbital is singly occupied. The low energy shoulder at $\lambda > 800 \text{ nm}$ is typical for Cu(II) in square pyramidal geometry.¹⁵ Using the Beer–Lambert law, the

value of molar absorption coefficient ε was found to be $150 \text{ L mol}^{-1} \text{ cm}^{-1}$, which is of similar magnitude to those calculated for other copper(II) complexes.¹⁶

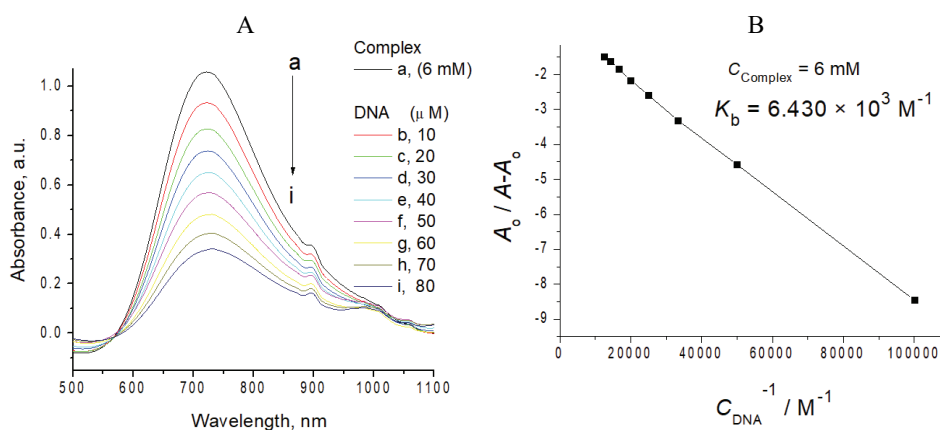


Fig. 6. A – Absorption peaks of the complex before (uppermost peak, peak a) and after DNA addition (lower peaks, peaks b-i) whereby the significant reduction in absorbance and the shift in λ_{max} on addition of DNA indicate complex–DNA interaction. B – the corresponding plot of $1/[\text{DNA}]$ vs. $A_0/(A-A_0)$ for calculation of K_b for the DNA added.

DNA binding study

The interaction of the complex with DNA was ascertained using four techniques.

Cyclic voltammetry. Since the concentration of electro-active complex is reduced on binding with DNA, there is a reduction in current on addition of DNA to the complex solution. Voltammograms of the complex were obtained before and after addition of DNA, as shown in Fig. 5. The decrease in current as a function of the incremental DNA addition was used to calculate the binding constant of the complex with DNA making use of the plot of $\log. I/(I_0-I)$ vs. $\log. 1/[\text{DNA}]$ which is shown in Fig. 7A. The value of the binding constant was $3.34 \times 10^3 \text{ M}^{-1}$, which is comparable to those of other copper(II) complexes.¹⁷ Moreover, the reduction in slope values of the anodic and cathodic peak currents vs. square root of the scan rate (shown in Fig. S-1 of the Supplementary material) indicated the formation of the complex–DNA adduct on addition of DNA to the complex solution. Likewise, the slope values of the plots of their logarithmic values are also reduced on addition of DNA, as shown in Fig. S-2 of the Supplementary material. Similarly, the reduction in peak current of the complex solution (3 mM) on addition of DNA was indicated by taking plots at various scan rates before and after DNA addition, as shown in Fig. S-3 of the Supplementary material. There was a shrinking of the current range as a result of addition of DNA to the complex solution, as evident from Fig. S-3B.

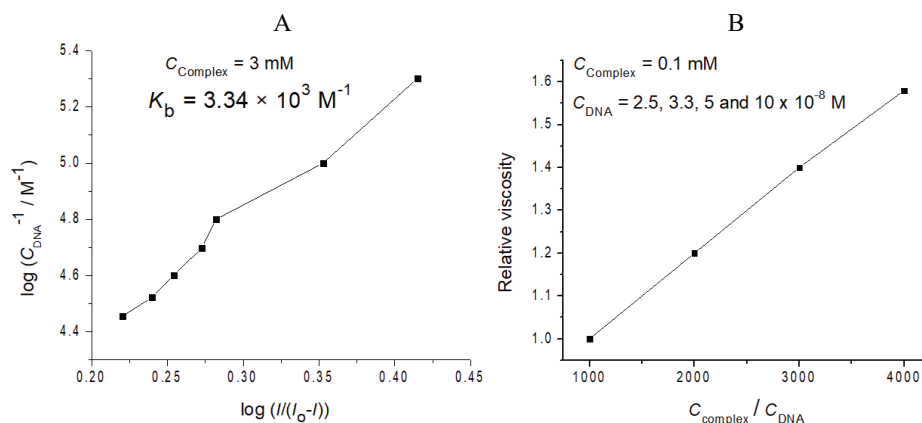


Fig. 7. A – Plot of the logarithmic values of the relative peak current vs. concentration of DNA (2, 8, 17, 23, 26, 30, 35, 44, 47 and 56 μM DNA) for calculation of K_b through cyclic voltammetry and B – plot of concentration of complex/concentration of DNA vs. relative viscosity showing that the viscosity of DNA increased steadily with increasing amount of complex added to the DNA solution.

Apart from the calculation of the DNA-binding constant, cyclic voltammetry was used to calculate the diffusion coefficient D_0 of the complex after DNA addition using the same procedure as that used before DNA addition. The D_0 value after DNA addition was calculated to be $1.770 \times 10^{-8} \text{ cm}^2 \text{ s}^{-1}$, which is smaller than that calculated, $3.032 \times 10^{-8} \text{ cm}^2 \text{ s}^{-1}$, before DNA addition. This shows a reduction in the active concentration of the complex on addition of DNA, which is further evidence of DNA interaction with the complex.

Absorption spectroscopy. The reduction in the concentration of the free complex on addition of DNA can be accessed through absorption spectroscopy as the addition of DNA to a solution of the complex resulted in diminution of the absorption of the complex, as shown in Fig. 6A. The reduction in absorbance as a function of DNA addition enables the calculation of the DNA-binding constant by employing the slope of a plot of $1/[\text{DNA}]$ vs. $A_0/(A-A_0)$ (shown in Fig. 6B) using the Benesi–Hildebrand equation.¹⁰ The value of the DNA-binding constant thus calculated was $6.90 \times 10^3 \text{ M}^{-1}$. The values of the DNA-binding constant of the complex determined through cyclic voltammetry and absorption spectroscopy were lower than the unsubstituted 2-phenylacetate copper(II) complex¹⁰ and another minor groove binder of the copper(II) complex.⁶ However, these values are comparable to some other copper(II) complexes $[\text{Cu}(\text{dipica})(\text{diimine})]^{2+}$, $[\text{Cu}(\text{L-tyrosine})(5,6\text{-dmp})]^{2+}$ and $[\text{Cu}(\text{imda})(\text{diimine})]$ complexes (dipica is di-2-picolylamine, 5,6-dmp is 5,6-dimethyl-1,10-phenanthroline and imda is imino-diacetate).^{18–20}

Viscometry. Interaction of the complex with DNA results in an alteration of the viscosity of a DNA solution. The viscosity of the DNA solution was mea-

sured in the absence and presence of different concentrations of complex and the values were plotted relative to the concentration of DNA, as shown in Fig. 7B. The plot shows that there was an increase in the relative viscosity of DNA with addition of the complex, indicating an overall lengthening of the DNA chain. This may be due to the insertion of complex into the base pairs of DNA.¹⁶

Competitive ethidium bromide assay. Ethidium bromide (EBr) is famous for its strong binding with DNA having fluorescence emission in the bound state. On addition of complex solution to EBr–DNA solution, the complex replaces the EBr molecules and binds itself with DNA, setting EBr free. Since the fluorescence intensity of the free EBr is quenched in the buffered medium, its replacement by complex is indicated by a reduction in the fluorescence intensity. Addition of 4, 7 and 10 μM complex caused 6.5, 29.5 and 75 % reduction in intensity of the EBr–DNA solution, respectively, as shown in Fig. 8. There is a linear reduction in fluorescence intensity of the EBr indicating binding ability of the complex with DNA.

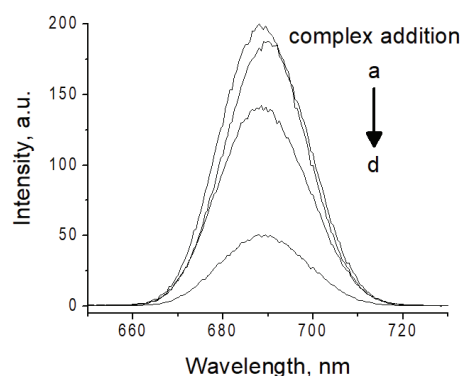


Fig. 8. Fluorescence emission spectra of equimolar ethidium bromide–DNA solution in the absence (uppermost peak, peak a) and presence (lower peaks, peaks b–d) of 4, 7 and 10 μM complex. The reduction in emission intensity of EBr indicates preferential binding of complex with DNA.

All the four techniques indicate potent DNA-binding ability of the synthesized complex.

Antifungal studies

The results showed that complex at concentration of 200 $\mu\text{g}/\text{mL}$ in DMSO exhibited significant activity against fungal strain *Mucor piriformis* (inhibiting 75 ± 4 % of its growth), moderate activity against *Aspergillus niger* (inhibiting 50 ± 3 % its growth) and insignificant activity against *Helminthosporium solani*. Terbinafine was taken as standard in this study which exhibited 100 % growth inhibition at concentration of 200 mg/mL . The complex indicated excellent activity against *Mucor piriformis* although its activity was lower than the standard used. This type of activity was observed for some other copper(II), nickel(II) and zinc(II) complexes derived from a pentadentate macrocyclic ligand.⁸ The reference complexes were active against some microbial strains but their activity was

lower than the standard used in that study. The behavior of the complex against the fungal strains is also typical of the other copper(II) complexes already reported where the complexes showed antifungal activity against some of the strains but were totally inactive against others.²¹ The antifungal activity of the synthesized complex is also better than the structural analogue derived from the unsubstituted 2-phenylacetate ligand studied against the same fungal strains and standard under the same reaction conditions.¹⁰

CONCLUSIONS

In summary, a less commonly found polynuclear complex of copper(II) metal was prepared and structurally characterized. The structure was found to be linear polymeric consisting of interlinked paddlewheel units without intervening ligands. The purity was assessed from a powder XRD study and its DNA binding ability from electrochemistry, absorption and fluorescence spectroscopic techniques and viscometry. The complex showed significant activity against fungal strain *Mucor piriformis*. The preliminary findings indicated excellent biological potency of the synthesized complex.

SUPPLEMENTARY MATERIAL

Additional data are available electronically from <http://www.shd.org.rs/JSCS/>, or from the corresponding author on request.

ИЗВОД

БИНАРНИ БАКАР(II) КОМПЛЕКС ПОЛИМЕРНЕ СТРУКТУРЕ: СИНТЕЗА, КАРАКТЕРИЗАЦИЈА, ДНК ИНТЕРАКЦИЈЕ И АНТИФУНГАЛНА АКТИВНОСТ

MUHAMMAD IQBAL¹, SAQIB ALI², MUHAMMAD N. TAHIR³, MUHAMMAD ABDUL HALEEM¹, HUSSAIN GULAB¹ и NASEER ALI SHAH⁴

¹Department of Chemistry, Bacha Khan University, Charsadda 24420, KPK, Pakistan, ²Department of Chemistry, Quaid-i-Azam University, Islamabad 45320, Pakistan, ³Department of Physics, University of Sargodha, Sargodha, Pakistan и ⁴Department of Biosciences, Islamabad Campus, COMSATS University Islamabad, Park Road, Islamabad, Pakistan

У реакцији између 2-(4-метилфенил)ацетата и бакар(II)-сулфата добијен је у квантитативном приносу полимерни бакар(II) комплекс необичне структуре. Комплекс је окарактерисан применом FT-IR, ESR и апсорпционе спектроскопије, као и електрохемијски и методом дифракције X-зрака са кристала и праха. Нађено је да се структура састоји од спојених пропелерских јединица без интервентног лиганда, што резултира у степеничастом полимерном распореду структуре. Чистоћа узорка је одређена на бази XRD података добијених са прахова, док је ESR спектроскопијом нађен слаб сигнал чија је вредност између 3000 и 4000 G, што указује на постојање Cu(II) јона у комплексу. Електрохемијска мерења указују на иреверзибилност углавном дифузионо контролисаног $\text{Cu}^{\text{II}}\text{Cu}^{\text{II}}/\text{Cu}^{\text{II}}\text{Cu}^{\text{I}}$ процеса, са израчунатом D_0 вредности од $3,032 \times 10^{-8} \text{ cm}^2 \text{ s}^{-1}$. Применом цикличне волтаметрије, апсорпционе и флуоресцентне спектроскопије, као и методом мерења вискозитета, испитивана је интеракција комплекса са ДНК, при чему су добијене следеће вредности за константе K_b : $3,34 \times 10^3$ и $6,90 \times 10^3 \text{ M}^{-1}$. Нађено је да испитивани комплекс показује значајну антифунгалну активност према соју *Mucor piriformis*, осредњу активност према *Aspergillus niger* и

слабу активност према соју *Helminthosporium solani*. Ови прелиминарни резултати тестова указују на значајан биолошки потенцијал синтетисаног бакар(II) комплекса.

(Примљено 23. априла, ревидирано 19 јуна, прихваћено 24. јуна 2019)

REFERENCES

1. M. A. Halcrow, *Chem. Soc. Rev.* **42** (2013) 1784 (<http://dx.doi.org/10.1039/c2cs35253b>)
2. M. Iqbal, S. Ali, A. Haider, N. Khalid, *Iran. J. Sci. Technol., Trans. A: Sci.* **42** (2016) 1859 (<http://dx.doi.org/10.1007/s40995-016-0141-5>)
3. M. Iqbal, S. Ali, M. N. Tahir, *Acta Chim. Slov.* **65** (2018) 131 (<http://dx.doi.org/10.17344/acsi.2017.3702>)
4. P. Smart, A. Bejarano-Villafuerte, L. Brammer, *CrystEngComm* **15** (2013) 3151 (<http://dx.doi.org/10.1039/C3CE26890J>)
5. R. Cl  rac, F. A. Cotton, K. R. Dunbar, E. A. Hillard, M. A. Petrukhina, B. W. Smucker, *C. R. Acad. Sci., Ser. IIc: Chim.* **4** (2001) 315 ([http://dx.doi.org/10.1016/S1387-1609\(01\)01233-6](http://dx.doi.org/10.1016/S1387-1609(01)01233-6))
6. U. Yildiz, B. Coban, *J. Serb. Chem. Soc.* **83** (2018) 1 (<https://doi.org/10.2298/JSC180802102Y>)
7. G. Sava, A. Bergamo, P. J. Dyson, *Dalton Trans.* **40** (2011) 9069 (<http://dx.doi.org/10.1039/c1dt10522a>)
8. E. Soleimani, S. A. N. Taheri, M. Sargolzaei, *J. Serb. Chem. Soc.* **82** (2017) 665 (<http://dx.doi.org/10.2298/JSC161206039S>)
9. I. Banerjee, P. N. Samanta, K. K. Das, R. Ababei, M. Kalisz, A. Girard, C. Mathoniere, M. Nethaji, R. Cl  rac, M. Ali, *Dalton Trans.* **42** (2013) 1879 (<http://dx.doi.org/10.1039/c2dt30983a>)
10. M. Iqbal, S. Ali, M. N. Tahir, *Z. Anorg. Allg. Chem.* **644** (2018) 172 (<http://dx.doi.org/10.1002/zaac.201700375>)
11. D. L. Reger, A. Debreczeni, B. Reinecke, V. Rassolov, M. D. Smith, R. F. Semeniuc, *Inorg. Chem.* **50** (2011) 4669 (<http://dx.doi.org/10.1021/ic200654n>)
12. I. Fomina, Z. Dobrokhotova, G. Aleksandrov, A. Bogomyakov, M. Fedin, A. Dolganov, T. Magdesieva, V. Novotortsev, I. Eremenko, *Polyhedron* **29** (2010) 1734 (<http://dx.doi.org/10.1016/j.poly.2010.02.021>)
13. J. Wang, *Analytical Electrochemistry*, 1st ed., VCH Publishers, Weinheim, 1994, pp. 165–166 (ISBN 1-56081-575-2)
14. A. J. Bard, L. R. Faulkner, *Electrochemical Methods, Fundamentals and Applications*, 2nd ed., Wiley, New York, 2004, p. 236
15. S. S. Massoud, F. R. Louka, Y. K. Obaid, R. Vicente, J. Ribas, R. C. Fischer, F. A. Mautner, *Dalton Trans.* **42** (2012) 3968 (<http://dx.doi.org/10.1039/C2DT32540C>)
16. M. Iqbal, S. Ali, M. N. Tahir, *J. Coord. Chem.* **71** (2018) 991 (<http://dx.doi.org/10.1080/00958972.2018.1456655>)
17. X. Wang, M. Yan, Q. Wang, H. Wang, Z. Wang, J. Zhao, J. Li, Z. Zhang, *Molecules* **22** (2017) 171 (<http://dx.doi.org/10.3390/molecules22010171>)
18. S. Ramakrishnan, M. Palaniandavar, *J. Chem. Sci.* **117** (2005) 179 (<https://doi.org/10.1007/BF03356114>)
19. S. Ramakrishnan, V. Rajendiran, M. Palaniandavar, V. S. Periasamy, B. S. Srinag, H. Krishnamurthy, M. A. Akbarsha, *Inorg. Chem.* **48** (2009) 1309 (<https://doi.org/10.1021/ic801144x>)
20. B. Selvakumar, V. Rajendiran, P. Uma Maheswari, H. Stoeckli-Evans, M. Palaniandavar, *J. Inorg. Biochem.* **100** (2006) 316 (<https://doi.org/10.1016/j.jinorgbio.2005.11.018>)
21. K. Alomar, A. Landreau, M. Allain, G. Bouet, G. Larcher, *J. Inorg. Biochem.* **126** (2013) 76 (<http://dx.doi.org/10.1016/j.jinorgbio.2013.05.013>).